Open access • Journal Article • DOI:10.1109/TFUZZ.2019.2957254

Fuzzy-Based Distributed Protocol for Vehicle-to-Vehicle Communication

— Source link

Ammar Hawbani, Esa Torbosh, Xingfu Wang, Peter Sincak ...+2 more authors

Institutions: University of Science and Technology of China, Technical University of Košice, Shenyang Aerospace University, Edinburgh Napier University

Published on: 01 Mar 2021 - IEEE Transactions on Fuzzy Systems (IEEE)

Topics: Fuzzy set, Fuzzy logic, Routing protocol, Network packet and Vehicular communication systems

Fuzzy based Distributed Protocol for Vehicle to Vehicle Communication

Ammar Hawbani, Esa Torbosh, Xingfu Wang, Peter Sincak, Liang Zhao, and Ahmed Al-Dubai

Abstract— this paper modeled the multihop data-routing in Vehicular Ad-hoc Networks(VANET) as Multiple Criteria Decision Making (MCDM) in four steps. First, the criteria which have an impact on the performance of the network layer are captured and transformed into fuzzy sets. Second, the fuzzy sets are characterized by Fuzzy Membership Functions(FMF) which are interpolated based on the data collected from massive experimental simulations. Third, the Analytical Hierarchy Process(AHP) is exploited to identify the relationships among the criteria. Fourth, multiple fuzzy rules are determined and, the TSK inference system is employed to infer and aggregate the final forwarding decision. Through integrating techniques of MCDM, FMF, AHP, and TSK, we designed a distributed and opportunistic data routing protocol, namely, VEFR (Vehicular Environment Fuzzy Router) which targets V2V (vehicle-to-vehicle) communication and runs in two main processes, Road Segment Selection(RSS) and Relay Vehicle Selection(RVS). RSS is intended to select multiple successive junctions through which the packets should travel from the source to the destination, while RVS process is intended to select relay vehicles within the selected road segment. The experimental results showed that our protocol performs and scales well with both network size and density, considering the combined problem of end-to-end packet delivery ratio and end-to-end latency.

Index Terms—vehicular network, analytical hierarchy process, TSK fuzzy inference system, fuzzy routing;

1 Introduction

THE explosive usage of mobile electronics and recent advances in telecommunications made the *Ad-hoc Vehicular Networks* (VANETs) a more attainable technology to meet the ever-increasing demands for improving the efficiency of *Intelligent Transportation Systems* (ITS). ITS aims to provide innovative services related to different modes of transport and traffic management, and enables users to be better informed and make safer, more coordinated, and smarter use of transport networks. To implement such innovative services and applications, a coherent communication among vehicles and an efficient routing mechanism should be developed by taking into account the network challenges such as rapid topology changes and spare vehicle densities. Besides, the routing mechanism should highly consider the quality of service (QoS) such as, increasing the end-to-end delivery ratio, reducing the end-to-end latency and minimizing the communication overhead [15].

Mostly, communications in VANETs are classified into *vehicle-to-vehicle* (V2V), *vehicle to infrastructure* (V2I), and *vehicle-to-anything (V2X)*. Each vehicle mounts a hardware device called *On-Board Unit* (OBU) that accesses the wireless channel through radio frequency antenna in order to communicate with other OBUs and *Road-side units* (RSUs) [32]. The OBU employs *Wireless Access in Vehicular Environment* (WAVE) that supports V2V and V2I with a channel width of 10MHz, frequency bands of 5.86-5.92GHz, bit rate of 3-27Mbps and a range of communication up to 1km. The RSU, on the other hand, has a wired interface to communicate with other RSUs and a wireless communication interface to communicate with OBUs mounted on vehicles. WAVE has high transmission power, and long-range antenna to access the wireless medium. The wireless interface of RSU runs the basic MAC/PHY layers functionalities defined by WAVE standard in which the PHY layer is described in IEEE 802.11p that relies on *Orthogonal Frequency Division Multiplexing* (OFDM) mechanism to support different data rates. The functionalities of the MAC layer, on the other hand, are described in IEEE 1906.4 standard that extends the *Enhanced Distributed Channel Access* (EDCA) paradigm to cover two channels operations [29]. To communicate with a global controller or station, each OBU has a wireless interface that runs *Long-Term Evolution* (LTE) with a channel width of 20MHz, frequency bands of 700-2600MHz, bit rate of 300Mbps and a range of communication up to 30km [32].

Multi-hop data routing with taking into account the QoS metrics such as high delivery rate, low latency, and low communication overhead is the key backbone for implementing VANET services and applications. By intensely exploring multi-hop mechanism in VANET, it can be effortlessly seen that there are multiple attributes (physical quantities or multiple criteria) that supervise the performance of the network layer. In fact, the routing decision (i.e., next hop vehicle, or next hop junction) is an aggregation function of multiple criteria. For instance, the *density* and *shortest distance* are the most common attributes that have been involved during selecting the next hop junction or road segment [34]. These attributes can be linguistically classified further into different measurements. For example, the density can be classified into *low*, *medium* and *high* while the distance can be classified into *close*, *medium* and *far*. These measurements make the routing decision fuzzier. In reality, the routing decision is extremely intuitive

- *A. H., Xingfu W. {anmande, wangxfu} @ustc.edu.cn, and Esa T. (esa2017 @mail.ustc.edu.cn) are with School of Computer Science and Technology, University of Science and Technology of China, Hefei, Anhui 230027, China;*
- *P. Sincak (peter.sincak@tuke.sk) is the head of department of Cybernetics and Artificial Intelligence in Technical University of Košice, Slovakia, European Union;*
- *L.Zhao (lzhao@sau.edu.cn); Shenyang aerospace University; Shenyang, 110136, China;*
- *A.Al-Dubai is with School of Computing; Edinburgh Napier University; (a.al-dubai@napier.ac.uk);*

when dealing with one attribute, since we need to pick up the alternative with the highest priority, e.g., the *shortest path* has the uppermost priority when the distance is considered as an attribute. However, the decision would be very sophisticated when multiple criteria are involved, since several conflicting objectives should be achieved simultaneously.

Motivated by the abovementioned explanations, we modeled the multi-hop data routing in VANET as *Multiple Criteria Decision Making*. The strength of *fuzzy logic* to imitate human reasoning and compute the degree of truth corresponding to each attribute and reflect the desired goodness (competency) of multiple attributes is exploited [4]. *Fuzzy Membership functions* and *fuzzy rules* are easy to modify to adapt different environments. This makes *fuzzy logic* a suitable computational model to delineate routing policies, especially for the networks with rapid variation topologies such as vehicular environments [25]. In contrast to classical set theory and classical reasoning, in which a proposition is true or false, the fuzzy reasoning represents the membership(truth) of an element belonging to a specific set [6].

In view of the aforementioned explanations, the data routing in VANET is modeled as a problem of aggregating multi-criteria such that the overall routing decision is inferred based on a set of rules [5]. To compute the routing decision, our main idea encapsulates four consecutive steps. First, we captured the attributes (criteria) that outline the network layer performance. Second, each attribute is translated to a *linguistic variable* with multiple items such that each item is represented by a *fuzzy set*. The *membership function* of each *fuzzy set* is interpolated by employing curve fitting techniques based on the data collected from our simulations. Third, considering that an important factor during determining the forwarding decision is the relationship between the criteria involved, we utilized the *Analytical Hierarchy Process(AHP)* [1][2] to identify the relations among the criteria involved and assign a weight for each criterion. Fourth and last, to obtain the *final forwarding decision*, we utilize the *TSK inference system* [3] to aggregate the sub-output of each attribute(criterion).

Therefore, the main novelties of our protocol and contributions of this article are as follows:

1) The *inter-path* (i.e., selecting a sequence of successive road segments) is modeled as a multi-objective function that aggregates multiple attributes, *density,* and *shortest distance*. On the first hand, the *density* is defined as a linguistic variable with three fuzzy sets: *Low*, *Medium* and *High*. Based on our statistical data and experimental simulations, the *Low* membership function is interpolated by *Boltzmann* distribution, the *Medium* density membership function is interpolated by *Gaussian* process and the *High* density membership function is interpolated by the cumulative function of *Weibull*. On the other hand, we defined the *distance* as a linguistic variable with three fuzzy sets, *Close*, *Medium* and *Far*. The corresponding membership functions of the three fuzzy sets are interpolated by *Boltzmann*, *Cauchy–Lorentz,* and *Weibull* distributions, respectively.
2) We model the intra-path (i.e., the process of selecting the relay vehicles on the selected road segment) as a multi-objective function, which is utterly driven by multiple attributes such as speed difference, movement direction of vehicles, signal fading or path loss and transmission distance. Each of these attributes is modeled as a fuzzy set independently. We defined a membership function for each fuzzy set by applying different interpolations such as *Hill function, Cauchy-Lorentz, Gumbel curve and logistic curve*. To identify the relations among the involved attributes in both the *intra-path* and *inter-path*, the *Analytical Hierarchy Process* is applied. To obtain the *final forwarding decision*, the *TSK inference system* is employed.
3) Based on *inter-path* and *intra-path* strategies introduced above, a distributed and opportunistic data routing protocol called VEFR (*Vehicular Environment Fuzzy Router*) which targets V2V (vehicle-to-vehicle) and integrates MCDM, FMF, AHP, and TSK is developed. To simulate *VEFR*, a new platform with a graphical user interface that provides a detailed visualization of simulation runs with lots of relevant pieces of information is developed. The source code is available online via the link [https://github.com/howbani/VEFR].

The rest of this work is organized as follows. Section 2 explains the related work. Section 3 explains the attributes that influence network layer, and also introduces the fuzzy sets for each attribute. Our protocol *VEFR* (*Vehicular Environment Fuzzy Router*) is explained in Section 4. The experiments and discussions are elucidated in Section 5. Finally, Section 6 concludes this work.

2 Related work

Different techniques have been used to design different routing protocols in VANET such as genetic algorithms [30], opportunistic algorithms [33], heuristic algorithms [7], probabilistic algorithms [19], game theory [21], network coding [10] [25] and network clustering [16] [9]. Furthermore, different protocols have been designed for network layer to attain different QoS services such as minimizing delay [8] [21] [23] [30], increasing link stability [15], minimizing communication cost [4], increasing delivery ratio [33], and security issues [24]. Regardless of techniques employed to infer the routing decision, the routing protocols are broadly classified into distributed protocols and centralized protocols. In the distributed protocols, the routing decision is independently taken in each vehicle. While in the centralized protocols, the information of network topology is collected in an entity where the routing decision should be taken. These two classes are briefly reviewed in the remainder of this section.

2.1 Distributed Approaches

The *route-discovery*, *opportunistic algorithm*, *network clustering,* and *network coding* are the most common techniques to design the distributed protocols. The *route-discovery* protocols discover a path from the source to destination vehicles before sending the data packet, which in turn, due to the rapid changes of VANET topology, imposes the network to generate a large number of redundant control packets and increases the communication overhead owing to blind flooding [12]. Besides, after encapsulating the data packet in the source, the position of the destination will be changed, which will most likely leads to noticeable packet loss. An example of *route-discovery* protocols is proposed in [13], in which the routing strategy is formulated as a *constrained optimization problem*, and the authors suggested AQRV (*Adaptive Quality of Service Routing*) as a solution based on *ant colony optimization*. Utilizing the forward and backward ants, AQRV selects road intersections and road segments that are fitful to QoS constraints including connectivity probability, packet delivery, and delay. Once segments selection process is finalized, the source vehicle in AQRV initiates data packet transmission directly over the explored backbone paths.

In contrast, the paths in *opportunistic protocols* are not predetermined. Instead of that, each hop is selected instantaneously and independently [17] [26] in a distributed manner. However, due to the high mobility of the vehicles, neighboring tables in each hop should be updated promptly, which increases the number of beacon packets to be exchanged in the network. The information included in a single beacon contains the node's ID together with its status, e.g., position, speed and heading [27]. An example of an *opportunistic protocol* is introduced in [17]. The authors presented an opportunistic forwarding scheme called BRAVE in which the next forwarder is reactively selected based on the shortest distance. BRAVE runs in two steps, spatial awareness, and opportunistic geographic routing. The spatial awareness allows the packet to select the road segment based on the local information and street map utilizing the Dijkstra's algorithm. After selecting the road segment, the geographic routing strategy is employed to forward the packet along the selected segment.

Network clustering is widely applied to reduce communication overhead during data routing. In [16], the authors proposed a clustering-based routing protocol. Their main idea is to classify the vehicles into four categories based on communication equipment. The four categories are VANET communication, mobile communication, satellite communication, and mobile communication together with satellite communication. The vehicle forwarders are prioritized based on three values, communication equipment, location, and velocity. The overall priority is formulated as the sum of the three values and the vehicle with the highest overall priority is selected as a cluster head. Another example of clustering routing is proposed in [9], called MoZo (***Mo**ving **Zo**ne*), which divides the network into distinct zones based on the movement similarity which is determined by the speed, timestamp, and movement direction. Each zone has a captain vehicle (cluster head) which is responsible for managing the information about other member vehicles as well as responsible for data packet dissemination. Furthermore, MoZo estimates vehicles positions based on the similarity of movement, and each captain estimates its members based on their relative positions while the members need not update the captain with their current position periodicity.

Network coding is broadly utilized to improve the broadcast efficiency and data scheduling in VANET. The authors in [10] applied network-coding in V2V communication at a two-way road network. Similarly, the authors [25] utilized Network coding to design a routing protocol for VANET by engaging interflow coding at common backbone vehicles for different traffic flows. The backbone vehicles are filtered using fuzzy logic with three membership functions, the velocity, density, and channel capacity.

2.2 Centralized Approaches

Generally, the network-wide topological information improves the routing decision during packet disseminating. However, rapid topology changes due to the higher mobility, uneven vehicle density in urban environments make the global topology information difficult to acquire. *Software Defined Networking* (SDN) as an emerging technology has the potential to resourcefully coordinate vehicle networks challenges as it has a logically centralized controller entity that enables a wide-ranging view of the network. SDN highly supports the dynamic nature of vehicular network functions and efficiently facilitates intelligent applications with various demands for QoS through a dramatic simplification of network configuration, resource management, and programmability. The rest of this subsection reviews a few studies that exploited SDN centralized approach.

HRLB (*Hierarchical Routing scheme with Load Balancing*) [28] proposed a hierarchical geography routing protocol for software defined vehicular networks (SDVN). The SDVN architecture in HRLB is quite simple, in which the data plane consists of vehicles with no roadside units. The control plane contains the base stations and the controllers. The data routing mechanism in HRLB executes through three steps, *Grid selection*, *Path selection*, and *Relays selection*. In the Grid selection, HRLB divides the target region into multiple small equal-size grids by taking into account the geographical location and discovers a successive sequence of grids with good connectivity based on a real-time grid vehicle density and historical vehicle transfer probability between the grids. In the path selection, taking into account the selected sequence of grids, two paths with minimal costs and load balancing are selected. In the Relays selection, a sequence of relay vehicles on each selected path are filtered according to vehicle utility to forward the packets. To achieve a real-time grid vehicle density, HRLB incurs too much communication overhead due to the frequent handover between the data plane (vehicles) and the control plane (SDN controller).

Hierarchical Distributed Software Defined Networking architecture (HDSDVN) is proposed in [15] and integrated a routing scheme with *Flow Instantiation* (FI). HDSDVN considered the *travel times* and *link stability* as two routing quantities to find multiple shortest paths to deliver a given number of packets. The *link stability* is computed based on the *link's capacity* which refers to the ability to deliver packets satisfying a minimum *Signal-to-noise ratio* (SNR). A link is considered to be terminated when the sensitivity level of the receiver does not reach (-82 dBm).

The authors in [14] proposed an SDN based service architecture to manage the heterogeneous resources of VANET in a centralized manner in order to make scheduling decision and data dissemination for the devices in the data plane. The heterogeneity of distinct wireless communication interfaces with different characteristics (i.e., communication range and transmission rate) were studied, as well as the heterogeneity of data items in terms of data size. Besides, like in [12] the vertical handovers (i.e., automatic switch from one wireless interface to another in order to maintain communication in heterogeneous VANET) was formulated as a multi-objective optimization problem and a coding-assisted algorithm was proposed as a solution.

3 Attributes and Fuzzifier

Generally, the performance of a routing protocol in V2V is tightly abutted on multiple attributes or multiple criteria, the terms attribute and criteria are interchangeably used in this paper. In our work, routing decision is aggregated by multi-criteria function [5]. To do so, this section introduces the attributes that influence the performance of VANET, and explains how to model each attribute using fuzzy logic. Based on the data collected from our simulation, we extracted multiple attributes that draw off the performance and QoS in the network layer. We defined each attribute as a linguistic variable such that each variable comprises multiple measurement items. Each item is modeled as a fuzzy set which is characterized by a corresponding fuzzy membership function. The membership function is interpolated by different curve fitting methods such as *Hill function, Cauchy-Lorentz, Gumbel curve and logistic curve*. To leverage the relationship among the attributes, *Analytical Hierarchy Process* (AHP) [2] is exploited. Finally, after determining the fuzzy rules, we utilized the TSK inference system [3] to infer the final *forwarding competency* from the rules.

Table 1: Notations.

Notation	Description
v_i; $r_{i,j}$; $\lambda_{i,j}$; (x_i, y_i); $\lvert r_{i,j}\rvert$;	$\mathcal{V}_\mathcal{G} = \{v_0, v_1, v_2, \dots, v_i\}$ represents road junctions. v_s denotes the source junction. Destination junction is denoted by v_b . $r_{i,j}$ denotes the segment joins two junctions $v_i, v_j \in \mathcal{V}_\mathcal{G}$; $\lambda_{i,j}$ denotes the arrival rate parameter. (x_i, y_i) denotes the location of junction v_i. $\lvert r_{i,j}\rvert$ denotes segment length.
$\acute{\rho}_{ij}$;δ;	$\acute{\rho}_{ij}$ denotes vehicles *special density;* δ denotes communication range.
$\mu_i^j(x)$	j denotes the linguistic variable, i denotes the fuzzy set, x denotes the crisp input.
n_i; $(\check{x}_i, \check{y}_i)$;	Vehicle i, located at $(\check{x}_i, \check{y}_i)$.
$d_{i,j}$	The distance between the vehicles n_i and n_j.
$\theta_{i,j}$	The direction angle between the junctions v_i and v_j.

In this work, the routing process in VANET roughly contains two main processes, *Road Segment Selection (RSS)* and *Relay Vehicle Selection(RVS)*. *RSS* is a centralized process which is based on aggregating multi-criteria function to make an overall decision that essentially considers the global-view of network topology. *RSS* makes the decision of selecting successive road segments (or junctions) in a distributed manner by considering two attributes (criteria) *valid distance* and *connectivity(density)*. This can be implemented by a fuzzy system that captures multiple fuzzy crisp inputs such as *direction angle*, *segment length*, *transmission range*, *number of lanes*, and the expected number of vehicles as shown in Fig.1. On the other hand, the *Relay Vehicle Selection(RVS)* is a distributed process which is computed based on aggregating multi-criteria to prioritize the relay vehicles. The overall decision function aggregates multiple constraint attributes, such as speed difference, moving direction, transmission distance and signal fading as shown in Fig.2. These two processes are explained in the follows two subsections.

3.1 Road Segment Selection (RSS)

We assume that the road network for a given city is modeled as a directed graph $\mathcal{G} = (\mathcal{V}_\mathcal{G}, \mathcal{E}_\mathcal{G})$, where $\mathcal{V}_\mathcal{G} = \{v_0, v_1, v_2, \dots, v_i\}$ is the set of vertices representing the road junctions, and $\mathcal{E}$ is the set of edges representing the road segments that join the junctions. The segment that joins two intersections $v_i, v_j \in \mathcal{V}_\mathcal{G}$ is denoted by $r_{i,j}$. The frequently used notations in this work are listed in Table 1.

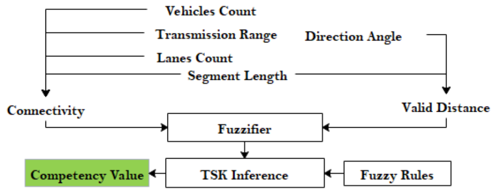

Fig.1: Structure diagram of the fuzzy logic proposed for RSS.

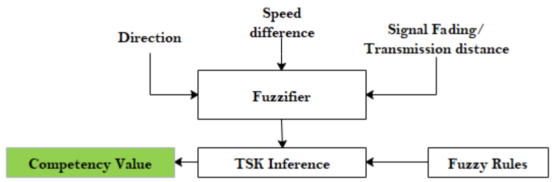

Fig.2: Structure diagram of the fuzzy logic proposed for RVS.

3.1.1 Road Segment Selection Attributes

As shown in Fig.1, the input variables for the RSS fuzzy system are the *valid distance* and *density*. *Shortest distance* from the source to the destination decreases the number of hops, which in turn truncates the delivery delay. However, the *shortest* distance is not always efficient because there could be no enough vehicles on the selected shortest segment to ensure connectivity. Similarly, a large number of vehicles improves the connectivity of network which in turn decreases the end-to-end delay, however, it induces a channel contention that leads to more packets collisions and hence the packets dropped. To tradeoff among these conflicting attributes, our protocol exploits fuzzy logic to resembles human reasoning and obtains a human decision-making from multiple attributes (criteria).

a) Density Attribute

Before modeling the density of road segment by using fuzzy logic, we will first find out the density input crisp. Segment connectivity is entirely correlated with vehicles density which is computed by combining multiple factors such as *inter-distance* of vehicles on the segment, transmission range of vehicle or roadside unit, number of lanes in the road segment, segment length and the number of vehicles. We Assume that each vehicle is equipped with OBU that holds a communication unit with a transmission range denoted by δ . Vehicle n_i is able to communicate with a subsequent vehicle n_j and relays the packet if the *inter-distance* of n_i and n_j does not exceed δ. Here, we define the vehicles *special density* $\acute{\rho}_{ij}$ by Eq.(1) where γ denotes the number of lanes and E_{ij}^{R} refers to the expected number of vehicles in the road segment $r_{i,j}$, $\bar{l}$ refers to the average length of the vehicle, and $R_{i,j}(k)$ is the probability that there are k vehicles reside within one lane in $r_{i,j}$.

$$\acute{\rho}_{i,j} \triangleq \frac{2.\gamma.E_{i,j}^{R}}{|r_{i,j}|}\ ;\ E_{i,j}^{R} = \sum_{x=0}^{|r_{i,j}|/\bar{l}} x.R_{ij}(x)\ ;\ R_{ij}(k) = \frac{(\lambda_{i,j}|r_{i,j}|)^k}{k!}\ e^{-\lambda_{i,j}|r_{i,j}|} \quad (1)$$

The arrival of vehicles to a specific road segment $r_{i,j}$ follows *Poisson* process with arrival *rate parameter* $\lambda_{i,j} = 1/\alpha_{i,j}$ that represents the number of arrivals in a second. The time difference between two successive arrivals (interarrival time in second) to the segment $r_{i,j}$ follows the exponential distribution with the *mean parameter* $\alpha_{i,j} > 0$, as in Eq.(2) where z_0 and z_1 are two uniformly generated numbers from the interval [0, 1]. The μ_I and σ_I are the *expected value* and the *standard deviation* of the *normal distribution*, respectively.

$$\alpha_{i,j} = \left|\mu_I + \left(\sigma_I\sqrt{-2\log z_0}\ \sin(2\pi z_1)\right)\right| \quad \forall r_{i,j} \in \mathcal{E}_{\mathcal{G}} \quad (2)$$

The road segment is virtually partitioned into $|r_{i,j}|/\delta$ blocks, that is the segment length divided by the communication range. Each block is δ meters in length. The probability that there are k vehicle(s) in a given block follows *Poisson* distribution, obtained by Eq.(3).

$$\hat{R}_{i,j}(k) = \frac{(\acute{\rho}_{i,j})^k}{k!}\ e^{-\acute{\rho}_{i,j}} \quad (3)$$

A block of segment is said to be connected if it occupied by at least one vehicle. Accordingly, the probability of existing at least one vehicle on a given block is obtained by Eq. (4).

$$\hat{R}_{i,j}(k > 0) = 1 - \hat{R}_{i,j}(0) = 1 - e^{-\acute{\rho}_{ij}} \quad (4)$$

Therefore, the road segment is said to be connected if all blocks are occupied, computed by Eq. (5). This value represents the input crisp of density.

$$\tilde{\xi}_{i,j} = \prod_{c=1}^{|r_{i,j}|/\delta} \left(1 - e^{-\acute{\rho}_{i,j}}\right) = \left(1 - e^{-\acute{\rho}_{i,j}}\right)^{\frac{|r_{i,j}|}{\delta}} \quad (5)$$

After characterizing segment density crisp as in Eq.(5), we define a linguistic variable $\mathcal{D}$ labeled by "*density*" to denote the segment density or connectivity. This variable includes three measurement items set $T(\mathcal{D})$ ={*Low, Medium, High*} as shown in Fig.3. Each item is modeled by a fuzzy set as follows. $\widetilde{\mathcal{D}}_L = \{(x, \mu_L^{\mathcal{D}}(x))|x \in [0,1]\}$ defines *Low* density, $\widetilde{\mathcal{D}}_M = \{(x, \mu_M^{\mathcal{D}}(x))|x \in [0,1]\}$ defines the fuzzy set of *Medium* density, and $\widetilde{\mathcal{D}}_H = \{(x, \mu_H^{\mathcal{D}}(x))|x \in [0,1]\}$ defines the fuzzy set of *High* density.

$$\mu_L^{\mathcal{D}}(x) = \begin{cases} \dfrac{1}{1 + e^{(x - x_0)/dx}} \\ x_0 = 0.25;\ dx = 0.05; \\ x = \tilde{\xi}_{i,j}\ ;\forall v_j \in \mathcal{V}_i \end{cases} \quad (6)$$

Based on data-set collected from massive experimental simulations, the *Low* density membership function $\mu_L^{\mathcal{D}}(x)$, as in Eq.(6), is interpolated by *Boltzmann* distribution, while the *Medium* density membership function $\mu_M^{\mathcal{D}}(x)$, as in Eq.(7), is interpolated by *Gaussian* process which is nonlinear interpolation that used for fitting a curve through discrete data.

The *High* density membership function $\mu_H^{\mathcal{D}}$, Eq.(8), is interpolated by the cumulative function of *Weibull* distribution.

$$\mu_M^{\mathcal{D}}(x) = \begin{cases} y_0 + \dfrac{A}{\sigma\sqrt{\pi/2}} e^{-2\frac{(x-\mu)^2}{\sigma^2}} \\ y_0 = 0.0338; A = 0.38289; \\ \mu = 0.5; \sigma = 0.30099; \\ x = \tilde{\xi}_{i,j}\ ;\forall v_j \in \mathcal{V}_i; \end{cases} \quad (7)$$

$$\mu_H^{\mathcal{D}}(x) = \begin{cases} \int_0^x b a^{-b} t^{b-1} e^{-\left(\frac{t}{a}\right)^b} dt = 1 - e^{-\left(\frac{x}{a}\right)^b} \\ x > 0; a = 0.66; b = 5; \\ x = \tilde{\xi}_{i,j}\ ;\forall v_j \in \mathcal{V}_i \end{cases} \quad (8)$$

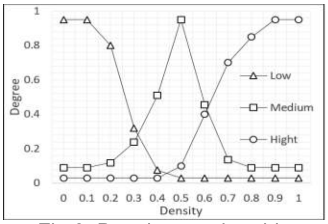

Fig.3: Density membership functions.

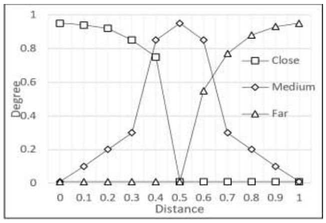

Fig.4: Valid distance membership functions.

b) Valid Distance Attribute

The intuition behind the concept of *Valid Distance* is the degree of closeness from source junction to the destination junction. The input crisp of *Valid Distance* $\widetilde{\Phi}_{i,j}$, as formulated in Eq. (9), is obtained by averaging the two values, direction angle, denoted by $\theta_{i,j}$, and the length of the segment, denoted by $\tilde{\mathcal{L}}_{i,j}$.

$$\widetilde{\Phi}_{i,j} = \begin{cases} \dfrac{A_1.\bar{\theta}_{i,j} + A_2.\tilde{\mathcal{L}}_{i,j}}{2} & \bar{\theta}_{i,j} \neq 1, A_1 = 0.4;\ A_2 = 0.6 \\ 1 & \text{otherwise} \end{cases} \quad \forall v_j \in \mathcal{V}_i; (9)$$

On the first hand, the *direction angle* $\theta_{i,j}$ between the current junction v_i and the potential next junction v_j towards the destination junction v_b is modeled as a dot production of two vectors $\vec{a}.\vec{c}$, such that $\vec{a} = (x_j - x_i, y_j - y_i)$ and $\vec{c} = (x_b - x_i, y_b - y_i)$ as formulated by Eq. (10) and normalized by Eq. (11).

$$\theta_{i,j} = cos^{-1}\left(\frac{(x_j - x_i)(x_b - x_i) + (y_j - y_i)(y_b - y_i)}{\sqrt{(x_b - x_i)^2 + (y_b - y_i)^2}\ \sqrt{(x_j - x_i)^2 + (y_j - y_i)^2}}\right) \quad (10)$$

$$\bar{\theta}_{i,j} = \begin{cases} \dfrac{\theta_{i,j}}{\pi} & 0^\circ \leq \theta_{i,j} \leq 90^\circ \\ 1 & \text{otherwise} \end{cases} \quad \forall v_j \in \mathcal{V}_i; (11)$$

On the other hand, the segment length is defined by *Euclidian* distance as shown in Eq. (12) where v_i represents the source junction and v_j represents the potential next junction towards the destination junction v_b.

$$\tilde{\mathcal{L}}_{i,j} = 1 - \left(1/\log\left(\sqrt{(x_j - x_i)^2 + (y_j - y_i)^2}\right)\right) \quad \forall v_j \in \mathcal{V}_i; (12)$$

After obtaining the input crisp of *Valid Distance* by Eq.(9) , we define "*valid distance*" as linguistic variable denoted by $\mathcal{H}$, as shown in Fig.4, with items set $T(\mathcal{H})$ = {*Close, Medium, Far*}. Each item correspondingly represents a fuzzy set as follows. $\widetilde{\mathcal{H}}_C$={ $(x, \mu_C^{\mathcal{H}}(x))|x \in [0,1]$} defines the *Close* fuzzy set where $\mu_C^{\mathcal{H}}(x)$ is the *Close* membership function which is interpolated by *Boltzmann* distribution as formulated by Eq.(13).

$$\mu_C^{\mathcal{H}}(x) = \begin{cases} \dfrac{1}{1+e^{(x-x_0)/dx}} \\ x_0 = 0.25;\ dx = 0.1; \\ x = \tilde{\Phi}_{i,j}\ ; \forall v_j \in \mathcal{V}_i \end{cases} \quad (13)$$

Similarly, the *Medium* fuzzy set is defined by $\widetilde{\mathcal{H}}_M$={ $(x, \mu_M^{\mathcal{H}}(x)) | x \in [0,1]$} where $\mu_M^{\mathcal{H}}(x)$ refers to the *Medium* membership function which is interpolated by *Cauchy–Lorentz* distribution as formulated by Eq.(14).

$$\mu_M^{\mathcal{H}}(x) = \begin{cases} y + \dfrac{2A}{\pi} \cdot \dfrac{w}{4(x-x_c)^2 + w^2} \\ y = -0.03785; x_c = 0.49537;\ w\ =\ 0.23932; \\ A\ =\ 0.3545;\ x = \tilde{\Phi}_{i,j}\ ; \forall v_j \in \mathcal{V}_i \end{cases} \quad (14)$$

The third fuzzy set $\widetilde{\mathcal{H}}_F$={ $(x, \mu_F^{\mathcal{H}}(x)) | x \in [0,1]$} defines the *Far* fuzzy set where $\mu_F^{\mathcal{H}}(x)$ is the *Far* membership function which is interpolated by the cumulative function of *Weibull* distribution as formulated in Eq.(15).

$$\mu_F^{\mathcal{H}}(x) = \begin{cases} \varphi.\left(1 - e^{-\left(\frac{x}{a}\right)^b}\right) \\ x > 0; a = 0.81; b = 5.11; \varphi = 0.9; \\ x = \tilde{\xi}_{i,j}\ ; \forall v_j \in \mathcal{V}_i \end{cases} \quad (15)$$

3.1.2 Road Segment Selection Inference

After using fuzzy logic to characterize and model the attributes, now we explain how to aggregate the selection decision of road segment based on a multi-criteria function. To this end, considering the density and the valid distance attributes, road segment selection rules are designed as listed in Table 2.

Table 2: Road segment selection rule-base

	Premise		Implication	
	Density	Valid Distance	Function	Aggregation
R 1	Medium	Close	$\mathbb{F}_1$	$\mathbb{G}_1$
R 2	Medium	Medium	$\mathbb{F}_2$	$\mathbb{G}_2$
R 3	Medium	Far	$\mathbb{F}_3$	$\mathbb{G}_3$
R 4	Low	Close	$\mathbb{F}_4$	$\mathbb{G}_4$
R 5	Low	Medium	$\mathbb{F}_5$	$\mathbb{G}_5$
R 6	Low	Far	$\mathbb{F}_6$	$\mathbb{G}_6$
R 7	High	Close	$\mathbb{F}_7$	$\mathbb{G}_7$
R 8	High	Medium	$\mathbb{F}_8$	$\mathbb{G}_8$
R 9	High	Far	$\mathbb{F}_9$	$\mathbb{G}_9$

We utilized TSK inference system [3] to infer the final *forwarding priority* from the rules shown in Table 2. The reason behind exploiting TSK is that the TSK inference system yields crisp outputs directly with no need for the defuzzification process. The consequences of the rules in TSK are polynomials. The rule has a premise part of membership function (*truth value)* denoted by $\mathbb{G}_i$ and a *linear polynomial function* denoted by $\mathbb{F}_i$ that implies the consequence for each rule when the premises are satisfied. Given a rule with k premises, TSK fuzzy models has the form as follows: R_i: **IF** x_1 is $\mu_i(x_1)$ **AND**…**AND** x_k is $\mu_i(x_k)$ **THEN** $\mathbb{F}_i(x_1, \dots, x_k)$=$w_0^i$+$w_1^i x_1$+$w_2^i x_2$+…+$w_k^i x_k$; The inputs $x_1 \dots x_k$ are the premises of the rule R_i while $\mu_i(x_1)$… $\mu_i(x_k)$ are the fuzzy sets associated with the rule. $\mathbb{F}_i$ denotes the consequent part which consists of the piecewise linear function. w_0^i…w_k^i are the constants and called the consequence parameters.

The determination of routing decision is firmly amalgamated with relationships among the criteria involved. To identify the relations among premises rules, a weight for each premise is obtained by employing *Analytical Hierarchy Process* (AHP) [2], which is an effective tool to deal with complex decision making by setting priorities for each attribute. The AHP is implemented by consecutive two steps, constructing a *pairwise comparison matrix* and *priority rating*. More details about these two steps can be found in [1]. Based on AHP, the *pairwise comparison matrix* $(m * m)$ is defined by Eq. (16), in which the entry a_{jk} represents the importance of the jth criteria relative to the kth. For example, the entry $a_{1,2} = 5$ means that the importance of *medium* density is five times compared to the *low* density. Note that $a_{jk}.\, a_{kj} = 1$. We included 6 sub-criteria in A^* such that each column contains six rows representing *Medium* density(M), *Low* density(L), *High* density(H), *Close* distance(C), *Medium* distance(MV) and *Far* distance(F). We derived the *normalized pairwise comparison matrix* such that each entry in A^* is normalized by Eq.(17). In the end, the criteria weight vector $\mathbb{W}$ =[*M, L, H, C, MV, F*] is obtained by averaging entries on each row on the *normalized pairwise comparison matrix* as formulated in Eq. (17).

$$A^* = \begin{bmatrix} / & / & M & L & H & C & MV & F \\ - & - & - & - & - & - & - & - \\ M & | & 1 & 5 & 4 & 1 & 2 & 7 \\ L & | & 1/5 & 1 & 1/2 & 1/6 & 1/2 & 1 \\ H & | & 1/4 & 2 & 1 & 1/3 & 1/2 & 2 \\ C & | & 1 & 6 & 3 & 1 & 5 & 7 \\ MV & | & 1/2 & 2 & 2 & 1/5 & 1 & 3 \\ F & | & 1/7 & 1 & 1/2 & 1/7 & 1/3 & 1 \end{bmatrix} \quad (16)$$

$$\bar{a}_{jk} = \frac{a_{jk}}{\sum_{l=1}^{m} a_{lk}}; w_k^i = \frac{\sum_{l=1}^{m} \bar{a}_{jl}}{m} \quad (17)$$

The inferred output of the TSK model with $z \geq 1$ rules each with $k \geq 1$ premises is obtained by Eq. (18). Note that $\mathbb{F}_i(x_1, \dots, x_k)$=$w_0^i$+$w_1^i x_1$+$w_2^i x_2$+…+$w_k^i x_k$ and $\mathbb{G}_i(x_1, \dots, x_k)$ is t-norm usually implemented as the *max* fuzzy operator.

$$\mathcal{R}_i(x_1, \dots, x_k) = \left(\sum_{i=1}^{z} \mathbb{G}_i(x_1, \dots, x_k). \mathbb{F}_i(x_1, \dots, x_k)\right)\left(\sum_{i=1}^{z} \mathbb{G}_i(x_1, \dots, x_k)\right)^{-1} \quad (18)$$

3.2 Relay Vehicle Selection(RVS)

The road segment selection is explained in the previous subsection. This subsection is dedicated to select the relay vehicles on the selected segment. We assume the location of the vehicle n_i is denoted by $(\check{x}_i, \check{y}_i)$. Given a vehicle n_i that has a transmission range of δ, the vehicles within the δ are considered as its neighbors, denoted by $\mathbb{N}_i$ (one-hop vehicles). By analyzing the RVS and based on data collected from our simulations, we concluded that the vehicle selection is influenced by multiple attributes such the transmission distance from the transmitter to receiver, the movement direction of vehicle, the speed difference between sender and receiver vehicles, and the memory size of OBU. We found the relationship between these attributes, and computed the membership corresponding to each attribute such that the desired competency of each attribute is acquired by a corresponding membership function.

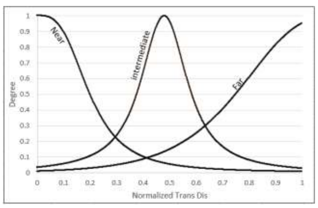

Fig.5: Transmission distance membership functions.

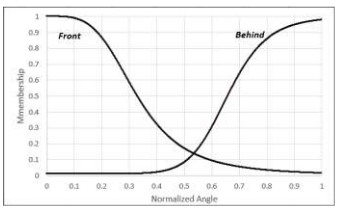

Fig.6: Moving direction membership functions.

3.2.1 Relay Vehicle Selection Attributes

a) Transmission Distance Attribute

The "*Transmission distance*" is defined as a linguistic variable denoted by $\mathcal{T}$ with items set $T(\mathcal{T})$ ={*Near, Intermediate, Far* } as shown in Fig.5. The *Intermediate* transmission distance from the transmitter to receiver is more desirable as it ensures a reliable communication link by avoiding *path-loss* which is the attenuation of signal power that occurs as a radio wave propagates over the distance. The *Far* transmission distance between the transmitter and receiver reduces the number of hops, but it largely increases *path-loss*. The *Near* transmission distance between the transmitter and receiver increases the number of hops and the communication overhead, but it ensures a reliable communication link. Based on these facts, we defined three fuzzy sets of transmission distance as follows. Note that the input crisp for *Transmission distance* is $x = \sqrt{(\check{x}_j - \check{x}_i)^2 + (\check{y}_j - \check{y}_i)^2}/\delta$.

$\tilde{\mathcal{T}}_N$ ={ $(x, \mu_N^{\mathcal{T}}(x)) | x \in [0,1]$ } defines the *Near* fuzzy set where $\mu_N^{\mathcal{T}}(x)$ represents the *Near* membership function which is interpolated by the modified *Hill function* with offset as formulated by Eq.(19).

$$\mu_N^{\mathcal{T}}(x) = \begin{cases} s + (\varepsilon - s)\dfrac{x^n}{k^n + x^n} \\ s = 1; \varepsilon = 0; k = 0.2;\ n = \pi; \\ x = \left(\sqrt{(\check{x}_j - \check{x}_i)^2 + (\check{y}_j - \check{y}_i)^2}/\delta\right) \end{cases} \quad (19)$$

The *Intermediate* fuzzy set is defined by $\tilde{\mathcal{T}}_I$ ={ $(x, \mu_I^{\mathcal{T}}(x)) | x \in [0,1]$ }, in which $\mu_I^{\mathcal{T}}(x)$ represents the membership function and interpolated by *Voigt* distribution which is a convolution of *Cauchy-Lorentz* distribution and *Gaussian* distribution as formulated in Eq.(20).

$$\mu_I^{\mathcal{T}}(x) = \begin{cases} y_0 + \left(\dfrac{2a}{\pi}\dfrac{w_l}{4(x - x_c)^2 + w_l{}^2}\sqrt{\dfrac{4Ln2}{\pi}}\dfrac{e^{-\frac{4Ln2}{w_g{}^2}x^2}}{w_g}\right) \\ y_0 = -0.00851; a = 0.3231; x_c = 0.4959; \\ w_l = 0.1916; w_g = 0.0617 \\ x = \left(\sqrt{(\check{x}_j - \check{x}_i)^2 + (\check{y}_j - \check{y}_i)^2}/\delta\right) \end{cases} \quad (20)$$

The *Far* fuzzy set is defined by $\tilde{\mathcal{T}}_F$={ $(x, \mu_F^{\mathcal{T}}(x)) | x \in [0,1]$} in which $\mu_F^{\mathcal{T}}(x)$ represents the degree of membership and interpolated by *Gumbel* distribution as formulated in Eq.(21).

$$\mu_F^{\mathcal{T}}(x) = \begin{cases} 1 - e^{-e^{(x-a)/b}} \\ a = 0.85; b = 0.16; \\ x = \left(\sqrt{(\check{x}_j - \check{x}_i)^2 + (\check{y}_j - \check{y}_i)^2}/\delta\right) \end{cases} \quad (21)$$

Note that the signal fading occurs due to the high mobility of surrounding vehicles, weather (particularly rain), or shadowing from obstacles affecting the radio wave propagation. The reflecting objects degrade the signal strength and the quality of the receiving signal. At the simulation level, the signal fading is modeled as *Nakagami-m* distribution, a continuous probability distribution that generalizes the small-scale fading for dense signal scatters and the radio wave propagation. The *probability density function* (pdf) of *Nakagami-m distribution* for a signal to be received with power x is formulated in Eq. (22) where $m \geq 1/2$ (*shape parameter*) represents the loss of signal intensity and the Ω controls the signal spread (*average power strength*).

$$f_m(x; m, \Omega) = \frac{m^m . x^{m-1} . e^{-(m/\Omega)x}}{\Omega^m . (m-1)!} \quad (22)$$

The *Cumulative Density Function* (CDF) is formulated in Eq. (23).

$$F_m(x; m, \Omega) = \int_0^x f_m(z; m, \Omega)\, dz = \frac{m^m}{\Omega^m (m-1)!}\int_0^x z^{m-1} e^{-(m/\Omega)z}\, dz \quad (23)$$

The probability that the packet has been received successfully is derived from the probability that the receiving power of the signal is greater than the threshold value r_x, formulated in Eq. (24).

$$Pr(x > r_x) = 1 - F_m(r_x; m, \Omega) = e^{-\frac{m}{\Omega}r_x}\sum_{i=0}^{m}\frac{\left(\frac{m}{\Omega}r_x\right)^{i-1}}{(i-1)!} \quad (24)$$

The Ω and r_x are derived from the *free-space model* as shown in Eq. (25) where T_p is the transmission power and $d_{i,j}$ is the distance between vehicles n_i and n_j; δ denotes the communication range while the antenna gain for the transmitter and receiver is denoted by G_t and G_r respectively; λ denotes the wavelength of the signal.

$$\Omega(d_{i,j}) = \frac{T_p}{d_{i,j}^2}G;\ r_x(\delta) = \frac{T_p}{\delta^2}\ ; G = \frac{G_t G_r \lambda^2}{16\pi^2} \quad (25)$$

The value of the *shape parameter* m , as mentioned in [35], is derived by Eq. (26).

$$m = \begin{cases} 1.0 & d_{i,j} \geq 150m \\ 1.5 & 50m \leq d_{i,j} < 150m \\ 3.0 & d_{i,j} < 50m \end{cases} \quad (26)$$

b) Moving Direction Attribute

Given a road segment $r_{s,d}$ =(v_s, v_d), where v_s denotes the start junction and v_d denotes the end junction. Let n_i be a vehicle holds a packet, and currently travels over an estimated position $(\check{x}_i, \check{y}_i)$ on the segment $r_{s,d}$. The current sender n_i selects one of its neighbors to be a relay. The relay vehicle $n_j \in \mathbb{N}_i$ should be in front of n_i without considering its heading direction(same direction of n_i or opposite direction). That is to say, the heading direction of the relay vehicle n_j is not important, since the packet should be traveled from the start junction v_s to the end junction v_d. Let $\vartheta \in [0,1]$ be the normalized angle between n_i to v_d and n_i the relay $n_j \in \mathbb{N}_i$ as formulated by Eq.(27). When $0 \leq \vartheta \leq 0.5$, the relay node n_j is located in front of n_i. Otherwise, n_j is located behind n_i.

$$\vartheta = cos^{-1}\left(\frac{(\check{x}_j - \check{x}_i)(x_d - \check{x}_i) + (\check{y}_j - \check{y}_i)(y_d - \check{y}_i)}{\sqrt{(x_d - \check{x}_i)^2 + (y_d - \check{y}_i)^2}\sqrt{(\check{x}_j - \check{x}_i)^2 + (\check{y}_j - \check{y}_i)^2}}\right)\Big/\pi \quad (27)$$

Let $\mathcal{M}$ be a linguistic variable with two items $T(\mathcal{M})$ ={*Front, Behind*} that defines the location of the relay vehicle related to the location of the sender vehicle. The two fuzzy sets $\tilde{\mathcal{M}}_F$ = $\{(x, \mu_F^{\mathcal{M}}(\vartheta)) | \vartheta \in [0,1]\}$ and $\tilde{\mathcal{M}}_B$=$\{(x, \mu_B^{\mathcal{M}}(\vartheta)) | \vartheta \in [0,1]\}$ define the *Front* and *Behind* fuzzy sets respectively, depicted in Fig.6. The *Front* $\mu_F^{\mathcal{M}}(\vartheta)$ and *Behind* $\mu_B^{\mathcal{M}}(\vartheta)$ membership functions are interpolated by *logistic curve* as formulated in Eq.(28) and Eq.(29), respectively. Note that ϑ is the crisp input, obtained by Eq.(27).

$$\mu_F^{\mathcal{M}}(\vartheta) = \begin{cases} \dfrac{1}{1 + \left(\frac{\vartheta}{x_0}\right)^p} \\ x_0 = 0.33;\ p = 3.8 \end{cases} \quad (28)$$

$$\mu_B^{M}(\vartheta)=\begin{cases}1+\dfrac{A_1-1}{1+\left(\frac{\vartheta}{x_0}\right)^p}\\ x_0=0.66;\ p=9.2;\\ A_1=0.01;\end{cases}\quad(29)$$

c) Speed Difference Attribute

The least speed difference between the sender and the receiver enhances network layer performance as it keeps the inter-distance between the two vehicles within the transmission range. This in turn allows more time to receive packets and reduces packet loss, especially when the size of the data packet is large. The vehicles with similar velocity stay longer together and closer to one another which reduces the beacon packets to be exchanged between them. The main goal of this attribute is to capture the similarity of speed such that a higher priority is assigned to the vehicle with the least speed difference. Let s_i, s_j and $max(s)$ be the speed of n_i, speed of n_j, and the maximum allowed speed, respectively. The speed difference crisp between the n_i and n_j is simply normalized by Eq.(28).

$$s_{i,j}=\left(\sqrt{\left(s_i-s_j\right)^2}\right)/max(s)\,;\forall\, n_j\in\mathbb{N}_i\quad(28)$$

Let $\mathcal{S}$ denotes the speed difference linguistic variable with three fuzzy sets $T(\mathcal{S})$ ={ *Small, Moderate, Large* } as plotted in Fig.7. We defined the *Small* difference fuzzy set by $\tilde{\mathcal{S}}_S$={ $(x,\mu_S^{\mathcal{S}}(x))|x\in[0,1]$} where $\mu_S^{\mathcal{S}}(x)$ is the membership function which is interpolated by *Boltzmann* distribution as formulated in Eq.(29).

$$\mu_S^{\mathcal{S}}(x)=\begin{cases}A_2+\dfrac{1-A_2}{1+e^{\frac{(x-x_0)}{dx}}}\\ dx=0.06;A_2=0.11;x_0=0.2;\\ x=s_{i,j}\,;\forall\, n_j\in\mathbb{N}_i\end{cases}\quad(29)$$

The *Moderate* speed difference is defined by the fuzzy set $\tilde{\mathcal{S}}_M$={ $(x,\mu_M^{\mathcal{S}}(x))|x\in[0,1]$} where $\mu_M^{\mathcal{S}}(x)$ is the membership function interpolated by *Gaussian* process, which is non-linear interpolation that used for fitting a curve through discrete data as formulated in Eq.(30).

$$\mu_M^{\mathcal{S}}(x)=\begin{cases}y_0+\dfrac{A}{\sigma\sqrt{\pi/2}}e^{-2\frac{(x-\mu)^2}{\sigma^2}}\\ y_0=-0.10857;A=0.6369;\\ \mu=0.5;\sigma=0.50166\\ x=s_{i,j}\,;\forall\, n_j\in\mathbb{N}_i\end{cases}\quad(30)$$

The *Large* speed difference is defined by the fuzzy set $\tilde{\mathcal{S}}_L$={ $(x,\mu_L^{\mathcal{S}}(x))|x\in[0,1]$} where $\mu_L^{\mathcal{S}}(x)$ is the membership function, interpolated by the *logistic curve* as formulated in Eq.(31).

$$\mu_L^{\mathcal{S}}(x)=\begin{cases}A_2+\dfrac{A_1-A_2}{1+\left(\frac{x}{x_0}\right)^p}\\ x_0=0.816;\ p=6.99;A_2=1.2;\\ A_1=0.09219;\ x=s_{i,j}\,;\forall\, n_j\in\mathbb{N}_i\end{cases}\quad(31)$$

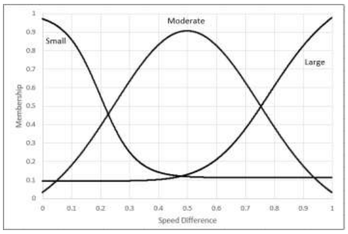

Fig.7: Speed difference membership functions.

3.2.2 Relay Vehicle Selection Inference

After using fuzzy logic to characterize and model the attributes that have an impact on selecting the relay vehicles, we will here explain how to aggregate the selection decision of relay vehicles based on a multi-criteria function. To this end, considering the *Transmission Distance*, *Moving Direction* and *Speed Difference* attributes, we designed relay vehicle selection rules as listed in Table 3. To infer the final forwarding priority, we feed the rules shown in Table 3 to *TSK inference system* that yields a crisp output directly without the defuzzification process, as explained above in RSS. To identify the relations among premises (*Transmission Distance*, *Speed Difference*, and *Moving Direction*) involved, we determined a weigh for each premise by employing the *Analytical Hierarchy Process*. The pairwise comparison matrix $(m*m)$ is defined by Eq. (32). We included 8 sub-criteria in A^* such that each column contains 8 rows representing *Near* transmission distance(N), *Intermediate* transmission distance (I), *Far* transmission distance (F), *Small* speed difference (S), *Moderate* speed difference (M), *Large* speed difference (L), *Front* moving direction(FR) and *Behind* moving direction(B).

$$A^*=\begin{bmatrix} / & / & N & I & F & S & M & L & FR & B\\ - & - & - & - & - & - & - & - & - & -\\ N & | & 1 & 3 & 5 & 1 & 2 & 5 & 1 & 5\\ I & | & 1/3 & 1 & 5 & 1/2 & 1 & 3 & 1/3 & 2\\ F & | & 1/5 & 1/5 & 1 & 1/5 & 1/3 & 1 & 1/4 & 2\\ S & | & 1 & 2 & 5 & 1 & 3 & 5 & 1 & 5\\ M & | & 1/2 & 1 & 3 & 1/3 & 1 & 3 & 1/4 & 2\\ L & | & 1/5 & 1/3 & 1 & 1/5 & 1/3 & 1 & 1/5 & 3\\ FR & | & 1 & 3 & 4 & 1 & 4 & 5 & 1 & 5\\ B & | & 1/5 & 1/2 & 1/2 & 1/5 & 1/2 & 1/3 & 1/5 & 1\end{bmatrix}\quad(32)$$

The inferred output of the TSK model with $z\geq 1$ rules each with $k\geq 1$ premises is obtained by Eq. (18).

Table 3: Relay vehicle selection rule-base

	Premise			**Implication**	
	TD	SD	MD	Function	Agg.
R 1	Near	Small	Front	$\mathbb{F}_1$	$\mathbb{G}_1$
R 2	Near	Small	Behind	$\mathbb{F}_2$	$\mathbb{G}_2$
R 3	Near	Moderate	Front	$\mathbb{F}_3$	$\mathbb{G}_3$
R 4	Near	Moderate	Behind	$\mathbb{F}_4$	$\mathbb{G}_4$
R 5	Near	Large	Front	$\mathbb{F}_5$	$\mathbb{G}_5$
R 6	Near	Large	Behind	$\mathbb{F}_6$	$\mathbb{G}_6$
R 7	Intermediate	Small	Front	$\mathbb{F}_7$	$\mathbb{G}_7$
R 8	Intermediate	Small	Behind	$\mathbb{F}_8$	$\mathbb{G}_8$
R 9	Intermediate	Moderate	Front	$\mathbb{F}_9$	$\mathbb{G}_9$
R 10	Intermediate	Moderate	Behind	$\mathbb{F}_{10}$	$\mathbb{G}_{10}$
R 11	Intermediate	Large	Front	$\mathbb{F}_{11}$	$\mathbb{G}_{11}$
R 12	Intermediate	Large	Behind	$\mathbb{F}_{12}$	$\mathbb{G}_{12}$
R 13	Far	Small	Front	$\mathbb{F}_{13}$	$\mathbb{G}_{13}$
R 14	Far	Small	Behind	$\mathbb{F}_{14}$	$\mathbb{G}_{14}$
R 15	Far	Moderate	Front	$\mathbb{F}_{15}$	$\mathbb{G}_{15}$
R 16	Far	Moderate	Behind	$\mathbb{F}_{16}$	$\mathbb{G}_{16}$
R 17	Far	Large	Front	$\mathbb{F}_{17}$	$\mathbb{G}_{17}$
R 18	Far	Large	Behind	$\mathbb{F}_{18}$	$\mathbb{G}_{18}$

4 Vehicular Environment Fuzzy Router

The main two processes of our protocol has been explained in the previous section. In this section, we will show how to apply these two processes to design a distributed and opportunistic multi-hops *vehicle-to-vehicle* (V2V) routing protocol called VEFR (*Vehicular Environment Fuzzy Router*). We assume that each vehicle is equipped with GPS receiver to obtain its geographic position and has an access to a street level digital map using an *onboard navigation sys-*

tem to determine the position of junctions and road segments [31].

4.1 Inter-path

The inter-path requires assistance from a centralized entity to compute the vehicles density. Vehicle applies inter-path process when approaching junctions (e.g., 30 meters to the heading junction), while the intra-path process is applied in the otherwise cases. The main goal of this process is to decide the next road segment that the packet should be switched to. The decision requires extra centralized info such as the location of the destination and the heading junction of destination. Such information is obtained by *Long-Term Evolution* (LTE). Let n_k be the current sender and is currently traveling on the segment $r_{x,i} = (v_x, v_i)$ (recall that v_x denotes the start junction and v_i denotes the heading junction). Vehicle n_k starts computing the next hop junction after acquiring road info via LTE wireless interface and before approaching the heading junction v_i. The inter-path algorithm computes next hop junction by the procedures outlined in **ALGORITHM 1**.

ALGORITHM 1: Inter-path.

Input: Given a vehicle n_k on the road segment $r_{x,i} = (v_x, v_i)$. $h(n_k)$ denotes the remain distance of the vehicle n_k to the heading junction v_i. $d(n_k)$ denotes the threshold distance to the heading junction v_i. Let v_b denotes the heading junction of destination vehicle.

Output: return $v_j \in \mathcal{V}_i$ such that v_j has the heights priority.

```
if h(n_k) ≤ d(n_k)
{
   ∀v_j ∈ V_i
   {
     Get the density crisp by Eq.(5);
     Get the valid distance crisp by Eq.(9);
     Classify the crisps, based on Table 4;
     Get the weight for each attribute based Table 4;
     Compute the priority for each junction by Eq. (18);
      and Eq. (16) by considering rules listed in Table 2;
   }
   return the junction with heights priority;
}
```

Table 4 shows the classifications and the weights of the fuzzy sets. For example, the vehicle density within the range (0~0.3) is considered as *low* and its *weight* is 0.054. The ranges are empirically obtained based on massive experimental and simulation results, while the weights are computed based on the *pairwise comparison matrix* as formulated in Eq. (16) and Eq. (32). The implementation of this algorithm is available online via the link [https://github.com/howbani/VEFR].

Vehicle starts switching the packet after selecting the road segment. However, it is not always possible to discover a relay vehicle around the intersection, causing the sender vehicle carries the packet instead of switching it to the appropriate segment. If the vehicle fails to switch the packet, VEFR will retry redirecting the packet to the selected segment. After 3 attempts, if the switching process fails, VEFR forwards the packet to the heading intersection, which means the packet will be traveled over an incorrect segment. This is still better than running out of retransmission attempts (7 times), which results in dropped packets.

Table 4: Crisps classification and attributes weight.

	Density			Moving Direction	
Item	Low	Medium	High	Front	Behind
Range	0~0.3	0.3~0.7	0.7~1	0~0.5	0.5~1
weight	0.054	0.313	0.092	0.233	0.037

	Valid Distance			Speed Difference		
Item	Close	Medium	Far	Small	Moderate	Large
Range	0~0.2	0.2~0.5	0.5~1	0~0.25	0.25~0.75	0.75~1
weight	0.3616	0.130	0.0443	0.216	0.09	0.040

	Transmission Distance		
Item	Near	Intermediate	Far
Range	0~0.32	0.32~0.62	0.62~1
weight	0.217	0.106	0.044

4.2 Intra-path

Intra-path is a distributed process, in which the sender vehicle selects next hop vehicle without any assistance from a centralized entity. Let $h(n_k)$ be the remain distance of the vehicle n_k to the heading junction v_i and let $d(n_k)$ be the threshold distance to the heading junction v_i. When a vehicle has a data packet and when $h(n_k) \geq d(n_k)$, the following procedures are followed. First, the vehicle broadcast a beacon packet to discover its neighbors. In case of no response to the broadcasted beacon, the vehicle employs *carry-and-forward* mechanism. That is to store the data for a predefined time (i.e., 3 seconds [9]) and retries to forward the packet again until reaching the maximum number of attempts (i.e., 7 attempts [33]). The data packet will be dropped if the maximum number of attempts is reached. Such a situation frequently ensues especially in the case of spare density, leading to network partition and, in consequence, the packet may not be further forwarded [18].

ALGORITHM 2: Intra-path.

Input: current vehicle n_i that holds the packet.

Output: a neighbor vehicle with heights priority.

```
if h(n_i) > d(n_i)
{
  if(N_i ≠ null) // N_i is the neighbor set of n_i.
  {
     ∀n_j ∈ N_i
     {
        Get Speed Difference by Eq.(28);
        Get Moving Direction by Eq.(27);
        Compute Transmission Distance d_{i,j}/δ;
        Classify the crisps, based on Table 4;
        Get the weight for each attribute based Table 4;
        Compute the priority for each vehicle by Eq. (18)
        and Eq. (32) by considering rules listed in Table 3;
     }
     return the neighbor vehicle with heights priority;
  }
  else store the packet in n_i;
}
```

On the other hand, in case that neighbor vehicles are discovered, the sender collects the info of the discovered neighbors including geolocation, speed, and heading junction (or moving direction). To select the next hop, the sender vehicle employs the intra-path (**ALGORITHM 2**) on discovered neighbors. The sender vehicle n_i selects the next hope vehicle in three steps. First, the elementary information such as speed and locations for all neighbor vehicles is collected through beacons packets. This information is converted into input crisps which are classified based on Table 4. Second, the degree of relationship of each attribute is obtained by injected the input crisps into the membership function of each fuzzy set. Third, the priority of each neighboring vehicle is computed based on the TSK inference, fuzzy rules listed in Table 3, and the weights listed in Table 4, as formulated by Eq. (18). The vehicle which has the highest priority will be selected as the next hop.

To reduce the overhead of neighbor discovery, VEFR utilizes *Neighbors Assortment* that keeps a track of the one-hop neighbors. *Neighbors Assortment* is a process to prioritize one hop vehicles according to their movement similarity which is computed by merging the speed difference, direction, and the signal fading. Vehicles with a higher similarity stay longer together and closer to each other and, consequently, the sender keeps them as neighbors in the routing table.

Our protocol VEFR adopts a flat structure (as in [33] and [17]) which means that no communication overhead to be incurred for maintaining or constructing clusters. However, VEFR incurs an overhead for neighbor discovery when a vehicle has a packet to send. Neighbor discovery starts by broadcasting a beacon packet to the surrounding one hop vehicles. The vehicles which have received the beacon packet send back an ACK packet to the sender. These vehicles are called *One-Hop Candidates* (OHC). The sender vehicle then selects one forwarder from the OHC to forward the data packet. This process is repeated until the data packet reaches its destination.

The overhead is computed as the number of beacon packets to be exchanged during the selection of the next hop vehicle, which is intimately related to the communication range and the vehicle density. To find the expected overhead, we count the number of receivers of beacon packets in each routing stage. This number can be easily obtained by counting the number of neighbors when the sender sends the beacon packet. The probability that there are k neighbors within the range of vehicle n_x is given by Eq.(33) and the expected communication overhead for one hop (denoted by $E[C_{hop}]$) is given by Eq. (34).

$$\zeta(k) = \frac{(\delta.\lambda)^k}{k!}\, e^{-\delta.\lambda} \quad (33)$$

$$E[C_{hop}] = \sum_{k=0}^{\infty} k.\zeta(k) = e^{-\delta.\lambda} \sum_{k=0}^{\infty} k.\frac{(\delta.\lambda)^k}{k!}$$
$$= \delta.\lambda\,.e^{-\delta.\lambda} \sum_{k=1}^{\infty} \frac{(\delta.\lambda)^{k-1}}{k-1!} = \delta.\lambda\,.e^{-\delta.\lambda} \sum_{j=0}^{\infty} \frac{(\delta.\lambda)^j}{j!}$$
$$= \delta.\lambda\,.e^{-\delta.\lambda}.e^{\delta.\lambda} = \delta.\lambda \quad (34)$$

Besides, the overhead for the routing path (denoted by $E[C_{path}]$) between the source and the destination is given by Eq. (35) where $E[H]$ is the expected number of hops between the source and destination vehicles, derived in [20].

$$E[C_{path}] = \delta.\lambda\,.E[H] \quad (35)$$

The mass function which reflects the probability of k hops between the source and the destination is given by Eq. (36) where $\mathcal{A}$ is the *border region*, obtained by Eq.(37). Further explanations about Eq. (37) are provided in [20].

$$\eta(k) = \left(e^{-\lambda\pi\delta^2(k-1)^2} - e^{-\lambda\pi\delta^2k^2}\right)\left(1 - e^{\lambda\mathcal{A}/2}\right)^{k-1} \quad (36)$$

$$\mathcal{A} = \delta^2.\left(\frac{\pi-2}{4}\right) + \mathcal{L}.\left(\theta - \frac{sin(2\theta)}{2}\right) \quad (37)$$

The expected number of hops between the source and destination vehicles is then given by Eq. (38).

$$E[H] = \sum_{k=0}^{\infty} k.\eta(k) = k\sum_{k=0}^{\infty}\left(\left(e^{-\lambda\pi\delta^2(k-1)^2} - e^{-\lambda\pi\delta^2k^2}\right)\left(1 - e^{\lambda\mathcal{A}/2}\right)^{k-1}\right) \quad (38)$$

5 Simulation And Results

This section is devoted to the performance evaluation of our proposed routing protocol VEFR. Extensive experimental simulations have been performed. Before reporting the simulation results, we introduce the simulation environment.

5.1 Simulation Environment

Due to the low support of graphical user interface and the low topology visualization in NS-3 (V3.28), which makes it really difficult to debug and design a high-level routing protocol in VANET, we developed a 2D simulation platform with a graphical user interface that provides detailed visualization and animation of simulation runs with lots of relevant pieces of information. The source code of our simulation platform is available online as an open-source project in the link：[https://github.com/howbani/VEFR]. The project was developed under the DOT NET 4.5 environment using C# and *Windows Presentation Foundation* (WPF) which is a graphical subsystem developed by *Microsoft* for rendering user interfaces in *Windows-based applications*.

Table 5: Simulation parameters.

Parameter	Default value
Network size	4000m×4500m.
Junctions	12 (Traffic light 5s).
Road segments	17 (2000m horizontal length, 1500m vertical length).
Speed	Maximum speed 90kmph and minimum speed 30kmph.
Packet size	1024 bytes for data packets 256 bytes for control packets.
Com. range	500m.
Model	V2V.
Distance	2000m (from the source to the destination).
Storing time	5s (when the network is partitioned).
Retransmission attempts	7 times for RTS, MAC DCF 802.11[33].
# vehicles	400.
Channel data rate	2Mbps.
Radio Propagation	*Nakagami-m*.

5.1.1 Experimental Settings

Road network size is set to 4000m×4500m with 12 junctions and 17 road segments (two roadways each with 2 lanes). The traffic light is set to 5 seconds. The starting position of vehicles is randomly distributed on the road network. Vehicles travel with a maximum speed of 90kmph and minimum speed of 30kmph. Note that the vehicles slow down when approaching the junctions and wait in a queue to make their turns. The *onboard unit* (OBU) employs IEEE 802.11p PHY/ IEEE 1906.4 MAC layers with a communication range of 500m for all vehicles. The packet size is set 1024 bits for the data packet while 256 bits for control packets. The default simulation parameters are listed in

Table 5.

5.1.2 Evaluation Metrics

Simulation results are reported by considering the following evaluation metrics:

- *Communication Overhead*. This counts the total number of control/data packets generated by vehicles all the way from the sources to destinations. Control packets include beacon for neighboring discovery, location query, and speed of neighbors, ACK packets and the packets that are intended to communicate with the local entity to obtain the road traffic and density through the *Long-Term Evolution* (LET) wireless interface.
- *End to end delay*. This accumulates the end-to-end time which is required to deliver the data packet from the source to the destination in seconds, including the carry-and-forward delay (when the network partitioned), queuing delay, propagation delay and processing delay.
- *Packets Success Ratio*. It expresses the ratio of the delivered packets to the generated packets in given simulation time.

5.1.3 Representative Approach for Comparison

The results of our protocol (VEFR) are compared to two different structure protocols, namely, clustering structure and flat structure. MoZo [9] is selected as an example of clustered protocols, while BRAVE [17] is selected as an example of flat-structure protocols. MoZo introduced similarity-score and assigned a higher score to the vehicle, which stayed together for longer and closer to each other. In addition, MoZo proposed moving zone, which has a large impact on reducing the overhead of communication. The next road segment selection in MoZo is calculated based on the shortest distance (*Dijkstra algorithm*), regardless of segment connectivity, which in turn largely leads to packet loss or slow packet delivery. Unlike MoZo, BRAVE is an opportunistic flat structure which eradicates the overhead of maintaining the hierarchical structure. BRAVE opportunistically performs hop-by-hop data relay based on greedy and geographic parameters, where the sender broadcasts the data packet and waits for neighboring vehicles that have received the data packet to respond with an ACK. The sender then selects the next forwarder based on the response time of ACK. For this reason, BRAVE generates higher overhead when selecting the next hop vehicle. In each hop selection in BRAVE, the data packet -not a beacon packet as in MoZo or in EVFR- is directly broadcasted which increases the network load. Besides, BRAVE selects the next hop based on the shortest distance regardless of the connectivity of the segment.

5.2 Experimental Results

Our compression results are concluded by varying three different evaluation scenarios, the distance between the source and destination vehicles, the number of vehicles, and the number of packets to be delivered, individually explained in the following three sub-sections. The reported result is the average of 10 independent runs of the same configurations.

5.2.1 Scenario 1: Varying The Distance

We set the number of vehicles to 400 by default, from which the source and destination vehicles are randomly selected. The number of source vehicles is set to 100, each source selects a destination randomly within x meters far such that the x is varied from 600 meters to 3500 meters, as in [9]. For each distance value, 100 packets are generated. The concluded results are as follows:

Delivery Delay. Evaluation results of delivery delay varying distance are shown in Fig.8. In most cases, the long distance between source and destination increases the number of hops, which in turn increases the packet delivery delay. Moreover, the longer distance increases the number of junctions between the source and destination, which in turn increases the number of packet switching at junctions which leads to more network partitions, since the sender vehicle may not discover a relay vehicle on the properly next selected segment. This raises carry-and-forward times and upsurges the delivery delay.

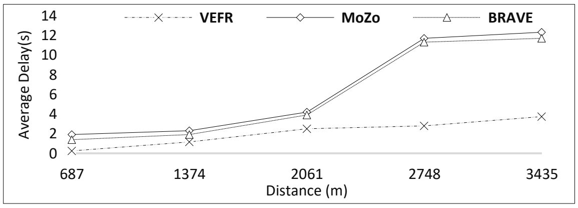

Fig.8: Latency varying distance.

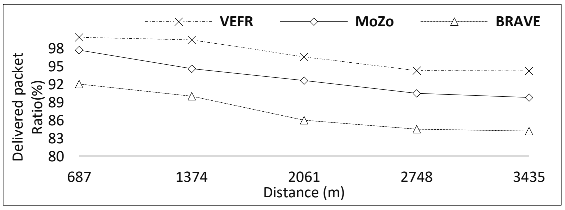

Fig.9: Success ratio varying distance.

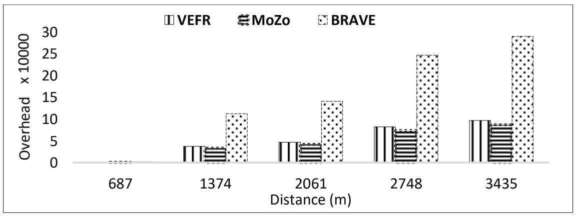

Fig.10: Overhead varying distance.

Form the reported results, we concluded that the flat structure protocols (VEFR and BRAVE) outperform the clustering structure (MoZo) because the flat structure does not need maintenance or construction. VEFR achieves the shortest delivery latency compared to BRAVE and MoZo for the following reasons. Both BRAVE and MoZo select the next road segment by considering the shortest distance (*Dijkstra algorithm*) regardless of the segment connectivity. The shortest distance is not always a good choice because there may be no vehicles on the shortest selected segment. In contrast, VEFR combined the shortest distance and road segment connectivity in a fuzzy multi-objective aggregation function which allows VEFR to infer the road segment priority based on TSK inference and the rules listed in Table 2. Besides, when selecting the next relay vehicle, BRAVE does not consider the speed difference and signal fading. MoZo selects the next forwarding vehicle within the zone (cluster) based on the shortest transmission distance (vehicle member near the next intersection) and considers the speed similarity during the zone construction. Due to the complexity of the cluster's maintenance and forwarding mechanisms, MoZo delivers packets slower than BRAVE because it needs to relay member's packets to the header (captain vehicle) and then from the captain to the next selected member, which results in longer latency. VEFR mimics human reasoning through inferring the final forwarding priority based on multiple criteria, transmission distance, speed difference, and moving direction. Forwarding priority in VEFR is inferred by feeding the rules (listed in Table 3) to TSK inference system.

Delivery Rate. The results of evaluating the delivery rate varying the distance are shown in Fig.9. Generally, for a given number of vehicles, greater distance from the source to destination decreases the delivery rate for the following reason. The network may encounter partitions causing the packet to be dropped. With longer distance, the probability of retransmission attempts gets greater and the packet will be dropped when the maximum number of retransmission attempts is exceeded (7 attempts). Also, the number of hops gets greater and the packet will be dropped if the time to live (TTL) or hop limit is exceeded. TTL is a mechanism that limits the lifespan of a packet in the network. Moreover, the probability of network partition is increased with longer distance due to various reasons such as the spare distribution of vehicles and packet switching at road junctions. Packet switching means that the sender vehicle switches the packet to the appropriate segment when approaching the heading junction. It is not always possible to discover a vehicle around the intersection to relay the packet, especially in the selected segment, so that the sender vehicle carries the packet instead of forwarding it to the appropriate segment.

VEFR overtakes BRAVE and MoZo due to *Inter-path* mechanism that drives the packets to travel over a shorter distance and an acceptable vehicle density. If the vehicle fails to switch the packet to the correct segment, VEFR will retry routing the packet to the selected segment. After 3 attempts, if the switching process fails, VEFR forwards the packet to the heading intersection, which means the packet will be traveled over an incorrect segment. Also, unlike BRAVE and MoZo, the proposed protocol VEFR abundantly exploits resources of the network. This is achieved by using vehicles in the same direction and in the opposite direction, which increases the packet delivery rate, especially in spare networks. MoZo shows better performance concerning the delivery rate than BRAVE because of the captain in MoZo contacts with more vehicles and, therefore, has a higher probability of retransmitting the packet before exhausting the retransition attempts. Retransmitting attempts are mostly exhausted due to packet switching at road junctions.

Communication Overhead. The results of evaluating the overhead varying the distance are shown in Fig.10. In general, for a given number of vehicles, the overhead grows as the distance between the source and the destination increases, since it is necessary to select more forwarders through multi-hops and then more operations need to be coordinated all the way. Furthermore, the process of packet switching is increased with longer distance, which in turn increases the overhead, especially when the packet is failed to be switched. Large overhead is incurred to redirect the packet to the right segment, especially, in MoZo and BRAVE since the two protocols enforce the packet to travel over the selected segment which exhausts the retransition attempts and drops the packet. VEFR and MoZo incurred almost the same overhead. BRAVE overhead is the highest since it broadcasts the data packet to all neighbors and then selects one of them to be the next forwarder. This routine is repeated from the source to the destination all the way. Although both VEFR and BRAVE are flat-structured, VEFR exhibits better performance, almost as good as clustering- based protocols. The main reason behind that is the *Neighbors Assortment* process that keeps the information of the neighbors based on the similarity score and, thus, it is not necessary to discover the neighbors periodically. Neighbors with higher similarity scores stay closer to the sender. MoZo showed lower overhead due to the clustering structure which reduces the communication among the cluster members. Members vehicles communicate directly with the captain vehicle and have no need for broadcasting. MoZo incurred most of the overhead to construct, maintain, merge and split the moving zones.

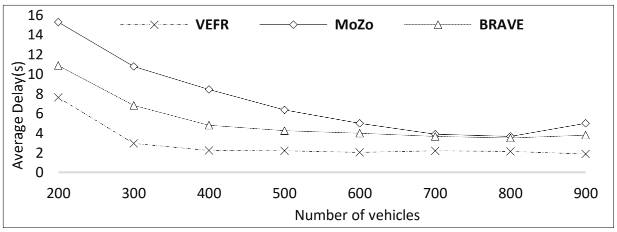

Fig.11: Delay varying number of vehicles.

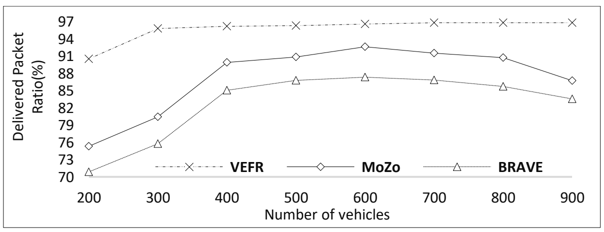

Fig.12: Delivery rate varying number of vehicles.

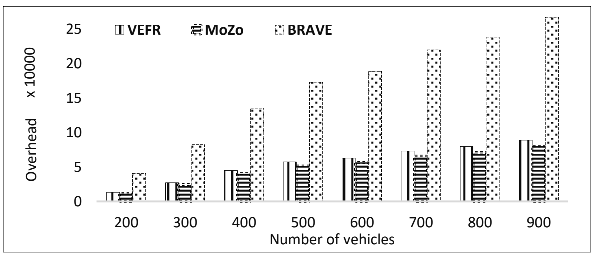

Fig.13: Total communication overhead varying number of vehicles.

5.2.2 Scenario 2: Varying Vehicles Number

The number of vehicles is varied between 200 and 900. The number of source vehicles is set to 100, each randomly selects a destination vehicle within 2000m and generates one packet.

Delivery Delay. The results of evaluating the latency varying the number of vehicles are plotted in Fig.11. In general, for a given size of a road network, a large number of vehicles improves network connectivity and reduces the number of *carry-and-forward*s, which in turn shortens latency. Besides, the higher density allows packets to travel primarily on selected segments, thus reducing switching failures of packets at junctions and reducing latency as well. With lower density, the network is often partitioned, which forces the vehicle to carry the packets and consequently takes longer to be disseminated.

VEFR decreases the number of *carry-and-forwards,* as it always selects the road segments with higher connectivity and shorter distance, which in turn, greatly decreases the probability of encountering network partition. This makes VEFR achieving lower latency compared to MoZo and BRAVE. In contrast, MoZo and BRAVE adopted *Dijkstra's algorithm* to select the shortest distance between the source and the destination. This is adopted without considering the connectivity of segment, which greatly increases the times of *carry-and-forward* and increases the end-to-end latency.

Delivery Rate. The results of evaluating packets delivery ratio varying the vehicles count are shown in Fig.12. It illustrates that for a given road network size, the delivery ratio grows with the number of vehicles. Packets are dropped when network is partitioned due to spare density. In MoZo and BRAVE, when the number of vehicles is between 200 and 600, the network connectivity increases and the probability of network partition decreases and hence the delivery ratio raises. On the other hand, when the number of vehicles is between 700 and 900, the network connectivity increases, however, it induces a channel contention problem that leads to more packets collisions and hence the packets are dropped. VEFR shows the best delivery rate over MoZo and BRAVE due to the selection of the next segment in inter-path and the selection of the next vehicle in the intra-path. These two selections counterbalanced network connectivity and traffic jam. MoZo has lower delivery rate than BRAVE since BRAVE generates more communication overhead and this leads to packets collisions in the wireless medium.

Communication Overhead. The results of evaluating the communication overhead varying the number of vehicles are shown in Fig.13. Obviously, the overhead grows up with the number of vehicles. In clustering-based structure (MoZo), the network overhead is increased, since more beacons will be generated to join or maintain the zones. On the other hand, in the flat based structure (BRAVE and VEFR), the overload will increase since the neighbors for each vehicle increase**.** MoZo and VEFR gain similar network overhead, lower than BRAVE. The main reasons behind that have been explained in Scenario 1.

5.2.3 Scenario 3: Varying Packets Count

This subsection evaluates VEFR's by varying the number of packets to be generated, from 100 to 500. The number of vehicles is set to 400 while the distance between the source and the destination is set to 2000m and all the packets are simultaneously generated.

Delivery Delay. The results of evaluating the delivery delay varying the number of packets to be generated are plotted in Fig.14. More road traffic increases the delivery time, especially the queuing delay. VEFR and BRAVE gain lower delivery time than MoZo for the same reasons explained in Scenario 1 and Scenario 2.

Delivery Rate. The results of evaluating the delivery rate varying the number of packets to be generated are shown in Fig.15. More road traffic decreases the delivery ratio due to the channel contention problem that leads to packet collisions. VEFR gains better performance over BRAVE and MoZo for the same reasons explained in Scenario 1 and Scenario 2.

Communication Overhead. The results of evaluating the communication overhead varying the number of packets to be generated are shown in Fig.16. More network traffic increases the network overhead. MoZo and VEFR gain similar network overhead, lower than BRAVE. The main reasons behind that are explained in the previous subsection.

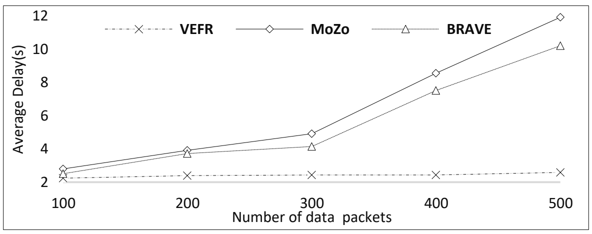

Fig.14: Average delay varying the number of data packets.

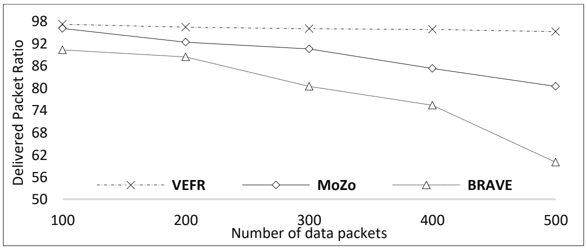

Fig.15: Delivery rate varying the number of data packets.

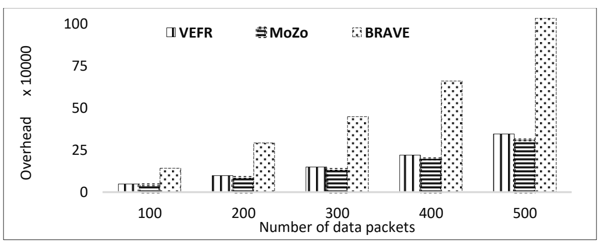

Fig.16: Total communication overhead varying the number of data packets.

6. Conclusion

This paper proposed a distributed routing protocol for vehicular urban environments, called VEFR (*Vehicular Environment Fuzzy Router*). VEFR models the routing problem as *Multiple Criteria Decision Making*(MCDM) by capturing the criteria which have a direct impact on the performance of the network layer. To model these criteria, VEFR utilized *fuzzy logic* while the *Analytical Hierarchy Process(AHP)* is exploited to identify the relationships among these criteria. Finally, the TSK inference system is employed to infer and aggregate the final forwarding decision based on the determined rules.

Acknowledgments

This paper is supported by the “Fundamental Research Funds for the Central Universities NO. WK2150110007 and WK2150110012” and by the National Natural Science Foundation of China (NO. 61772490, 61472382, 61472381, 61701322 and 61572454).

References

[1] Li, Caixia, Sreenatha Gopalarao Anavatti, and Tapabrata Ray. "Analytical hierarchy process using fuzzy inference technique for real-time route guidance system." IEEE Transactions on Intelligent Transportation Systems 15, no. 1 (2013): 84-93.

[2] Liao, Huchang, Xiaomei Mi, Zeshui Xu, Jiuping Xu, and Francisco Herrera. "Intuitionistic fuzzy analytic network process." IEEE Transactions on Fuzzy Systems 26, no. 5 (2018): 2578-2590.

[3] Takagi, Tomohiro, and Michio Sugeno. "Fuzzy identification of systems and its applications to modeling and control." In Readings in Fuzzy Sets for Intelligent Systems, pp. 387-403. Morgan Kaufmann, 1993.

[4] Li, Gen, Maode Ma, Chunfeng Liu, and Yantai Shu. "Adaptive fuzzy multiple attribute decision routing in VANETs." International Journal of Communication Systems 30, no. 4 (2017): 3014.

[5] Yager, Ronald R. "On ordered weighted averaging aggregation operators in multicriteria decisionmaking." IEEE Transactions on systems, Man, and Cybernetics 18, no. 1 (1988): 183-190.

[6] Minhas, Mahmood R., Sathish Gopalakrishnan, and Victor CM Leung. "Fuzzy algorithms for maximum lifetime routing in wireless sensor networks." In IEEE GLOBECOM 2008-2008 IEEE Global Telecommunications Conference, pp. 1-6. IEEE, 2008.

[7] Quan, Wei, Nan Cheng, Meng Qin, Hongke Zhang, H. Anthony Chan, and Xuemin Shen. "Adaptive transmission control for software defined vehicular networks." IEEE Wireless Communications Letters (2018).

[8] Deng, Der-Jiunn, Shao-Yu Lien, Chun-Cheng Lin, Shao-Chou Hung, and Wei-Bo Chen. "Latency control in software-defined mobile-edge vehicular networking." IEEE Communications Magazine 55, no. 8 (2017): 87-93.

[9] Lin, Dan, Jian Kang, Anna Squicciarini, Yingjie Wu, Sashi Gurung, and Ozan Tonguz. "MoZo: A moving zone based routing protocol using pure V2V communication in VANETs." IEEE Transactions on Mobile Computing 16, no. 5 (2016): 1357-1370.

[10] Liu, Fang, Zhiyong Chen, and Bin Xia. "Data dissemination with network coding in two-way vehicle-to-vehicle networks." IEEE Transactions on Vehicular Technology 65, no. 4 (2016): 2445-2456.

[11] Song, Tao, et al. "A cluster-based directional routing protocol in VANET." Communication Technology (ICCT), 2010 12th IEEE International Conference on. IEEE, 2010.

[12] Liu, Kai, Joseph KY Ng, Victor Lee, Sang H. Son, and Ivan Stojmenovic. "Cooperative data scheduling in hybrid vehicular ad hoc networks: VANET as a software defined network." IEEE/ACM Transactions on Networking (TON) 24, no. 3 (2016): 1759-1773.

[13] Li, Guangyu, Lila Boukhatem, and Jinsong Wu. "Adaptive quality-of-service-based routing for vehicular ad hoc networks with ant colony optimization." IEEE Transactions on Vehicular Technology 66.4 (2017): 3249-3264.

[14] Dai, Penglin, Kai Liu, Xiao Wu, Yong Liao, Victor Chung Sing Lee, and Sang Hyuk Son. "Bandwidth efficiency and service adaptiveness oriented data dissemination in heterogeneous vehicular networks." IEEE Transactions on Vehicular Technology 67, no. 7 (2018): 6585-6598.

[15] Liyanage, Kushan Sudheera Kalupahana, Maode Ma, and Peter Han Joo Chong. "Link stability based optimized routing framework for software defined vehicular networks." IEEE Transactions on Vehicular Technology (2019).

[16] Mohammed Nasr, Mohammed, Abdeldime Abdelgader, Zhi-Gong Wang, and Lian-Feng Shen. "VANET clustering based routing protocol suitable for deserts." Sensors 16, no. 4 (2016): 478.

[17] Ruiz, Pedro M., et al. "Brave: Beacon-less routing algorithm for vehicular environments." Mobile Adhoc and Sensor Systems (MASS), 2010 IEEE 7th International Conference on. IEEE, 2010.

[18] He, Jianping, et al. "Delay analysis and routing for two-dimensional VANETs using carry-and-forward mechanism." IEEE Transactions on Mobile Computing 16.7 (2017): 1830-1841.

[19] Yang, Shixin, Jing Liu, and Xiongshi Yan. "Flexible Routing-Proactive Updating Mechanism for Software Defined Vehicle Networks." In 2018 10th International Conference on Wireless Communications and Signal Processing (WCSP), pp. 1-6. IEEE, 2018.

[20] Rao, Ram Shringar, et al. "A probabilistic analysis of path duration using routing protocol in VANETs." International Journal of Vehicular Technology 2014 (2014).

[21] Li, He, Mianxiong Dong, and Kaoru Ota. "Control plane optimization in software-defined vehicular ad hoc networks." IEEE Transactions on Vehicular Technology 65, no. 10 (2016): 7895-7904.

[22] Sudheera, KL Kushan, Maode Ma, GG Md Nawaz Ali, and Peter Han Joo Chong. "Delay efficient software defined networking based architecture for vehicular networks." In 2016 IEEE International Conference on Communication Systems (ICCS), pp. 1-6. IEEE, 2016.

[23] Ghafoor, Huma, and Insoo Koo. "CR-SDVN: A cognitive routing protocol for software-defined vehicular networks." IEEE Sensors Journal 18, no. 4 (2017): 1761-1772.

[24] Weng, Jia-Si, Jian Weng, Yue Zhang, Weiqi Luo, and Weiming Lan. "BENBI: Scalable and dynamic access control on the northbound interface of SDN-based VANET." IEEE Transactions on Vehicular Technology 68, no. 1 (2018): 822-831.

[25] Wu, Celimuge, Satoshi Ohzahata, Yusheng Ji, and Toshihiko Kato. "How to utilize interflow network coding in VANETs: A backbone-based approach." IEEE Transactions on Intelligent Transportation Systems 17, no. 8 (2016): 2223-2237.

[26] Karagiannis, Georgios, et al. "Vehicular networking: A survey and tutorial on requirements, architectures, challenges, standards and solutions." IEEE communications surveys & tutorials 13.4 (2011): 584-616.

[27] Nizar Alsharif, and Xuemin Shen. "iCAR-II: Infrastructure-Based Connectivity Aware Routing in Vehicular Networks." IEEE Transactions on Vehicular Technology 66.5 (2017): 4231-4244.

[28] Gao, Yangshui, Zhilong Zhang, Dan Zhao, Yi Zhang, and Tao Luo. "A Hierarchical Routing Scheme with Load Balancing in Software Defined Vehicular Ad Hoc Networks." IEEE Access 6 (2018): 73774-73785.

[29] Ahmed, Shereen AM, Sharifah HS Ariffin, and Norsheila Fisal. "Overview of wireless access in vehicular environment (WAVE) protocols and standards." Indian Journal of Science and Technology 6, no. 7 (2013): 4994-5001.

[30] Lin, Chun-Cheng, Hui-Hsin Chin, and Wei-Bo Chen. "Balancing latency and cost in software-defined vehicular networks using genetic algorithm." Journal of Network and Computer Applications 116 (2018): 35-41.

[31] Saleet, Hanan, et al. "Intersection-based geographical routing protocol for VANETs: a proposal and analysis." IEEE Transactions on Vehicular Technology 60.9 (2011): 4560-4574.

[32] Saini, Mukesh, Abdulhameed Alelaiwi, and Abdulmotaleb El Saddik. "How close are we to realizing a pragmatic VANET solution? A meta-survey." ACM Computing Surveys (CSUR)48, no. 2 (2015): 29.

[33] Zhang, Xinming, Xulei Cao, Long Yan, and Dan Keun Sung. "A street-centric opportunistic routing protocol based on link correlation for urban VANETs." IEEE Transactions on Mobile Computing 15, no. 7 (2015): 1586-1599.

[34] Li, Gen, Maode Ma, Chunfeng Liu, and Yantai Shu. "Fuzzy multiple attribute decision routing in VANETs." In 2014 IEEE International Conference on Communication Systems, pp. 564-568. IEEE, 2014.

[35] Ma, Xiaomin, et al. "MAC and application-level broadcast reliability in vanets with channel fading." Computing, Networking and Communications (ICNC), 2013 International Conference on. IEEE, 2013.

Ammar Hawbani is an associate professor of networking and communication algorithms in the School of Computer Science and Technology at the University of Science and Technology of China, China. He received the B.S., M.S. and Ph.D. degrees in Computer Software and Theory from the University of Science and Technology of China (USTC), Hefei, China, in 2009, 2012 and 2016, respectively. From 2016 to 2019, he worked as Postdoctoral Researcher in the School of Computer Science and Technology at USTC. His research interests include IoT, WSNs, WBANs, WMNs, VANETs, and SDN.

Esa Torbosh received his B.S. degree in 2014 from Hefei University of Technology, Hefei, China in electrical engineering and automation. M.S. degree in 2017 from Hefei University of Technology, Hefei, China in Electrical engineering and automation. Currently, he is a Ph.D. student in School of Computer Science and Technology at USTC. His research interests include Vehicular Ad hoc Network.

Xingfu Wang received the B.S. degree in electronic and information engineering from Beijing Normal University of China in 1988, and the M.S. degree in computer science from the University of Science and Technology of China in 1997. He is an associate professor in the School of Computer Science and Technology, University of Science and Technology of China. His current research interests include Information Security, Data Management and WSN.

Peter Sincak received the M.S. Degree in 1984 and Dr. Eng. Degree from the Czech Academy of Science, Prague in 1992. He is a Marie Curie Research Alumni and currently is a full AI professor at Technical University of Kosice, Slovakia, European Union from 2002. He is Head of Department of Cybernetics and Artificial Intelligence, and his main areas of interest are Neural Networks, Fuzzy Systems for Classification and Cloud-based Artificial Intelligence or better Digital Intelligence.

Liang Zhao [M] is an associate professor at Shenyang Aerospace University, China. He received his Ph.D. degree from the School of Computing at Edinburgh Napier University in 2011. Before joining Shenyang Aerospace University, he worked as an associate senior researcher in Hitachi (China) Research and Development Corporation from 2012 to 2014. His research interests include VANETs, SDVN, FANETs, and WMNs.

Ahmed ADubai [SM] is Professor of Networking and Communication Algorithms in the School of Computing at Edinburgh Napier University, UK. He received the Ph.D. degree in Computing from the University of Glasgow in 2004. His research interests include Communication Algorithms, Mobile Communication, Internet of Things, and Future Internet.